An Information Theoretical Analysis of Nanoscale Molecular Gap Junction Communication Channel Between Cardiomyocytes

Deniz Kilinc, *Student Member, IEEE*, and Ozgur B. Akan, *Senior Member, IEEE*

***Abstract*—Molecular communication (MC) is a promising paradigm to communicate at nanoscale and it is inspired by nature. One of the MC methods in nature is the gap junction (GJ) communication between cardiomyocytes. The GJ communication is achieved by diffusion of ions through GJ channels between the cells. The transmission of the information is realized by means of the propagation of the action potential (AP) signal. The probabilities of both the AP propagation failure and the spontaneous AP initiation are obtained. For the first time in the literature, the GJ communication channel is modeled and analyzed from the information theoretical perspective to find the communication channel capacity. A closed-form expression is derived for the capacity of the GJ communication channel. The channel capacity, propagation delay, and information transmission rate are analyzed numerically for a three-cell network. The results of the numerical analyses point out a correlation between an increase in the incidence of several cardiac diseases and a decrease in the channel capacity, an increase in the propagation delay, and either an increase or a decrease in the transmission rate. The method that we use and results that are presented may help in the investigation, diagnosis, and treatment of cardiac diseases as well as help in the design of nanodevices communicating via GJ channels.**

***Index Terms*—Cardiac disease, cardiomyocyte, gap junction(GJ), molecular communication(MC).**

I. Introduction

NANOSCALE communication between nanodevices (e.g., engineered organisms or artificial devices) is a novel and interdisciplinary concept including nanotechnology, biotechnology, and communication technology [1]. The construction of nanonetworks by interconnecting nanodevices expands the capabilities of single nanodevices by means of cooperation between them [2]. The realization of the communication between nanodevices can be achieved through electromagnetic, acoustic, or molecular communication (MC) [3], [4]. The MC concept is defined as the information transmission using molecules and it is inspired by nature [5]. Several nature-inspired and theoretically modeled MC techniques exist in the literature based on pheromones [5], flagellated bacteria and catalytic nanomotors [2], pollen and spores [5], and Förster resonance energy transfer [6].

In this paper, for the first time in the literature, the nanoscale MC between ventricular cardiomyocytes is modeled and analyzed based on the information theory to obtain the communication channel capacity. The communication between the cardiomyocytes is achieved by the transmission of ions through channels in specialized structures of the cell membrane called gap junctions (GJs) [7]. This type of communication is called GJ communication and the GJ communication approach has been proposed for the communication of nanodevices [8]. The potential models for the GJ communication of nanodevices can be engineered from commonly used techniques such as GJ transfection of cultured HeLa cells with connexin coding DNAs or injection of Xenopus oocytes with connexin coding RNAs [9]. Therefore, the construction of the GJ communication channel is an existing technique used widely in physiology experiments. Unlike most of the existing models in the literature, this study presents information theoretical model of an already experimented, physically realizable and hence, realistic nanoscale communication channel. The model presented in this paper may help in investigation, diagnosis and treatment of cardiac diseases. Furthermore, the model can be utilized in the design and engineering of the GJ communication for nanodevices.

The rest of this paper is organized as follows. Section II presents the physical model of the GJ communication. In Section III, an information theoretical model of the GJ communication channel is proposed. Section IV presents a numerical analysis of the channel capacity, the channel propagation delay and the information transmission rate. In Section V, relations between cardiac diseases and the channel capacity, the propagation delay and the information transmission rate are discussed. This paper is concluded in Section VI.

II. Physical Model of GJ Communication

In the myocardium, i.e., the muscular tissue of the heart, the communication between two cardiomyocytes is achieved by the diffusion of ions at the cell-to-cell contact domain called gap junction (GJ) through pipe-like channels clustered in the GJ known as GJ channels [7]. The nanoscale MC between two cardiomyocytes is called GJ communication. For the rest of this paper, the GJ channels and the GJ communication

Manuscript received May 9, 2012; revised October 18, 2012; accepted December 3, 2012. Date of publication December 10, 2012; date of current version March 6, 2013. This work was supported in part by the Turkish Scientific and Technical Research Council under Grant 109E257, in part by the Turkish National Academy of Sciences Distinguished Young Scientist Award Program, and in part by IBM through IBM Faculty Award. The review of this paper was arranged by Associate Editor C. A. Moritz.

The authors are with the Next-Generation and Wireless Communications Laboratory, Department of Electrical and Electronics Engineering, Koc University, Istanbul, 34450, Turkey (e-mail: dkilinc@ku.edu.tr; akan@ku.edu.tr).

Color versions of one or more of the figures in this paper are available online at http://ieeexplore.ieee.org.

Digital Object Identifier 10.1109/TNANO.2012.2233212

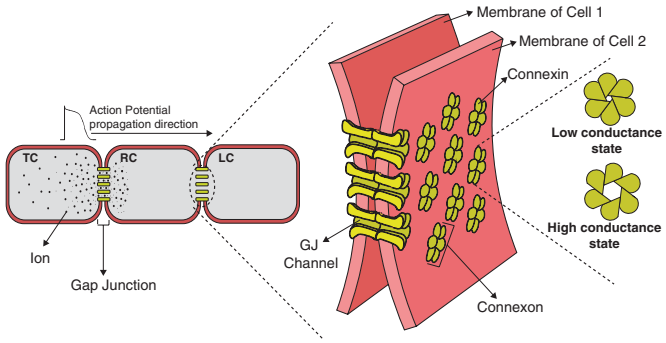

Fig. 1. Model of the GJ communication and GJ channels. The AP wave propagates by diffusion of ions through the GJ channels.

channel should not be confused with each other since the former refers to *the physical channels* clustered in a GJ while the latter refers to *the communication channel* formed by the GJ channels clustered in a GJ. To avoid any ambiguity between the physical channels and the communication channel, the communication channel is always denoted by *the GJ communication channel* and the physical channels are denoted by *the GJ channels*. In Fig. 1, a GJ forming a GJ communication channel between two cardiomyocytes and several GJ channels clustered in a GJ are shown.

In the GJ communication, the diffusion of ions between cardiomyocytes provides the propagation of the electrical activity called cardiac action potential (AP). The AP is initiated by the sinoatrial node, i.e., the impulse-generating tissue of the heart, and is used for the transmission of the information between cardiomyocytes [7]. That is, the information indicating whether cardiomyocytes contract or relax is encoded in the AP pulse train by the sinoatrial node. A cardiomyocyte at rest contracts when an AP pulse is successfully received, which is called excitation–contraction coupling. In contrast, when there is no AP pulse received by a cardiomyocyte, the corresponding cardiomyocyte stays at rest.

A basic network model of the GJ communication is shown in Fig. 1. In this model, APs are transmitted by a single transmitter caridomyocyte (TC), propagated through the GJ by means of the diffusion of the ions, and received by a single-receiver cardiomyocyte (RC). The ions diffused from TC to RC continue to diffuse to adjacent unstimulated cardiomyocytes, and this affects the AP initiation at the RC. To have a more realistic GJ communication model, there is also a loading cardiomyocyte (LC) to capture the loading effects of the unstimulated myocytes connected to the RC in the cardiac fiber. TC, RC, and LC are identical. In addition, according to the properties of both cardiomyocytes and the AP propagation stated previously, the GJ communication between cardiomyocytes is considered as a binary digital communication with On–Off Keying (OOK) modulation. That is, an AP pulse is considered as binary bit 1 and its absence is considered as binary bit 0.

A. Action Potential Propagation

The AP initiation in cardiomyocytes is described as follows. If a stimulus causes the membrane potential, i.e., the potential difference across the membrane of the cardiomyocyte, to become less negative than a threshold level, then the sodium (Na^+) channels embedded in the membrane open and allow Na^+ ions to enter the cardiomyocyte. This makes the membrane potential to rise causing depolarization of the membrane. As the membrane voltage rises, Na^+ channels close due to a process called inactivation. Next, calcium (Ca^{2+}) and potassium (K^+) channels open, which causes the membrane potential to stay constant; that is, the inward Ca^{2+} current and the outward K^+ current compensate each other for a while. Then, Ca^{2+} channels close but K^+ channels are still open causing rapid repolarization of the membrane. Finally, the membrane potential is restored to around -85 mV [10].

The potential difference between the stimulated and the unstimulated adjacent cardiomyocytes causes the ions to drift through the GJ channels leading the synchronous propagation of the AP. That is, the GJ coupling enables the wave of the AP to propagate from one cardiomyocyte to a neighbor cardiomyocyte by means of diffusion of the ions through the GJ channels. The AP propagation model assumes that each cardiomyocyte is isopotential, i.e., the membrane potential of each individual cardiomyocyte is the same over its membrane surface [11]. According to the model, the most important factor of the AP propagation is delay for an AP to pass through GJs. For the ion current flowing through the cardiomyocyte membrane, the current balance equation is

$$C_m S \frac{dv_n}{dt} = \frac{1}{R_{\mathrm{gj}}}(v_{n+1} - 2v_n + v_{n-1}) + SI_m \qquad (1)$$

where v_n is the membrane potential for the nth cell in one dimensional cardiac fiber, i.e., the potential difference between inside and outside of the cardiomyocyte, C_m is the membrane capacitance per unit area of the cardiomyocyte membrane, S is the surface area of the membrane, R_{gj} is the total GJ resistance between the cardiomyocytes, and I_m specifies the ionic currents per unit area of the membrane [10].

The most important deduction that can be extracted from (1) is that the propagation fails if R_{gj} is sufficiently large. That is, an increase in R_{gj} causes a decrease in the number of the diffused ions. The less number of ions may not be enough to increase the membrane potential of RC above the threshold value. The critical GJ resistance between TC and RC is denoted by R^*_{gj} and RC has an infinite voltage threshold if $R_{\mathrm{gj}} > R^*_{\mathrm{gj}}$. In [11], an expression is given for R^*_{gj} as

$$R^*_{\mathrm{gj}} = L\sqrt{\frac{\Gamma R_m}{S}}\left[\frac{E_2^2 - 2\mu_2 E_2 + 1}{(1-E_2^2)\sqrt{\alpha_2}} + \left(\frac{V_2 - V^*}{V_1 - V^*}\right)\frac{E_1^2 - 2\mu_1 E_1 + 1}{(1-E_1^2)\sqrt{\alpha_1}}\right] \qquad (2)$$

where R_m is the membrane resistivity, V_1 is the resting potential of the cardiomyocyte membrane, V_2 is the sodium equilibrium potential, V^* is the activation threshold voltage for Na^+ current, L is the length of the cardiomyocyte. Γ, E_1, and E_2 are variables defined as $\Gamma = (R_i/V_i) + (R_e/V_e)$ and $E_k = \exp\left(\sqrt{(\alpha_k \Gamma L^2 S)/R_m}\right)$ for $k = 1, 2$ where R_i and R_e are the cytoplasmic and extracellular medium resistivity values,

respectively, V_i is the volume of the cytoplasm of the cardiomyocyte, and V_e is the volume of the extracellular medium that surrounds the cardiomyocyte in the myocardium. The parameter values in (2) are taken as $V_1 = -87\,\text{mV}, V_2 = 28.8\,\text{mV}$, $V^* = -34.8\,\text{mV}, \alpha_1 = 1$, and $\alpha_2 = 108$ [12]. μ_1 and μ_2 satisfy the equality $R^*_{\text{gj}} = R_{\text{gj}}$ where R_{gj} is

$$R_{\text{gj}} = 2L\sqrt{\frac{\Gamma R_m}{\alpha_k S}}\frac{\left(\mu_k - \frac{1}{E_k}\right)(\mu_k - E_k)}{\mu_k\left(E_k - \frac{1}{E_k}\right)}, \quad k = 1, 2. \tag{3}$$

Numerical result of R^*_{gj} is found by solving two nonlinear equations which are $R^*_{\text{gj}} = R_{\text{gj}}$ for $k = 1$ and $R^*_{\text{gj}} = R_{\text{gj}}$ for $k = 2$. The upper limit of the GJ resistance for the successful propagation is R^*_{gj}, since the AP propagation strictly fails if $R_{\text{gj}} > R^*_{\text{gj}}$ as stated previously.

B. Physical Model of Gap Junction Channels

The GJs include the GJ channels that form a connection between neighboring cells in many tissues and organs providing chemical and electrical MC [7]. The physical structure of a GJ channel is formed by two hemichannels called connexons and they are embedded in the membrane of the connected cells. Each hemichannel includes six transmembrane proteins called connexins that are oligomerized in a hexameric structure to form a pore. Two hemichannels belonging to adjacent cells interact to form a complete GJ channel. The structure of GJ channels in a GJ can be seen in Fig. 1. The GJ channels have an evident selectivity for particle passage based on the permeability of the GJ channels and size of the particles. Thus, the AP propagation between cardiomyocytes depends on the permeability of the GJ channels since the diffusion of the ions is affected by the permeability of the GJ channels.

According to the stochastic behavior of the GJ channels [13], a GJ channel has two voltage-sensitive gates in series and one gate is located in each hemichannel. The channel gates control the GJ permeability and each gate has two states: an open state resulting in a high conductance and a closed state resulting in a low conductance for a hemichannel [13] as shown in Fig. 1. The voltage-sensitive gates control the channel conductance state in accordance to junctional voltage, i.e., potential difference between the membrane potentials of two adjacent cardiomyocytes denoted by V_j, in a stochastic manner. At any instant a GJ channel can be in any one of four states: *HH state*: both gates are open, *HL state*: one gate is open and the other gate is closed, *LH state*: one gate is open and the other gate is closed, and *LL state*: both gates are closed. The occurrence of the LL state, however, is very rare [14] and such a state has a very small conductance compared with the other states; thus, we choose to include only the first three states by neglecting the LL state. The stochastic dynamics of the GJ channels given in [13] is described by probabilities of a channel being in any of HH, HL, and LH states, denoted by $p_{\text{HH}}, p_{\text{HL}}$, and p_{LH}, respectively, given as

$$\begin{aligned}\frac{dp_{\text{LH}}}{dt} &= \beta_1(V_j)\cdot p_{\text{HH}} - \alpha_1(V_j)\cdot p_{\text{LH}}\\ \frac{dp_{\text{HL}}}{dt} &= \beta_2(V_j)\cdot p_{\text{HH}} - \alpha_2(v_j)\cdot p_{\text{HL}}\end{aligned} \tag{4}$$

where V_j is the junctional voltage and $p_{\text{HH}} + p_{\text{LH}} + p_{\text{HL}} = 1$. $\alpha_1(V_j), \alpha_2(V_j), \beta_1(V_j)$ and $\beta_2(V_j)$ are the rate constants of the state transitions which are

$$\begin{aligned}\alpha_1(V_j) &= \lambda\exp(-A_\alpha(V_j - V_0))\\ \alpha_2(V_j) &= \lambda\exp(A_\alpha(V_j + V_0))\\ \beta_1(V_j) &= \lambda\exp(A_\beta(V_j - V_0))\\ \beta_2(V_j) &= \lambda\exp(-A_\beta(V_j + V_0))\end{aligned} \tag{5}$$

where V_0 is the junctional voltage at which the opening and closing rates of the GJ channel gates have the same common value λ, and A_α and A_β are constants that indicate the sensitivity of a GJ channel to the junctional voltage [13]. Since connexin43 GJ protein is the major GJ protein in the ventricular muscle [15], in the numerical analysis, we use data obtained experimentally for the connexin43 GJ protein. Thus, we use the constants as $\lambda = 0.69, A_\alpha = 0.04(\text{mV})^{-1}, A_\beta = 0.07(\text{mV})^{-1}$, and $V_0 = 62\text{mV}$ [16].

C. Action Potential Propagation Failure

The conductance of each GJ channel, denoted by G_{ch}, is a random variable whose probability mass function is

$$f_G(G_{\text{ch}}) = \begin{cases} p_{\text{HH}}, \text{ if } G_{\text{ch}} = G_{\text{HH}} \\ p_{\text{HL}}, \text{ if } G_{\text{ch}} = G_{\text{HL}} \\ p_{\text{LH}}, \text{ if } G_{\text{ch}} = G_{\text{LH}} \end{cases} \tag{6}$$

where $G_{\text{HH}}, G_{\text{HL}}$, and G_{LH} are the conductance values of a single GJ channel in the respective state [13]. In this study, we use the GJ channel conductance values as $G_{\text{HH}} = 73\,\text{pS}, G_{\text{HL}} = 12\,\text{pS}$, and $G_{\text{LH}} = 12\,\text{pS}$, which are experimental results for connexin43 type GJ protein [15]. Since the GJ channels in a GJ are connected in parallel, the total conductance of the GJ having $n_{\text{HH}}, n_{\text{HL}}$, and n_{LH} GJ channels in HH, HL, and LH states, respectively, is given as

$$G_{\text{gj}}(V_j) = n_{\text{HH}}\cdot G_{\text{HH}} + n_{\text{HL}}\cdot G_{\text{HL}} + n_{\text{LH}}\cdot G_{\text{LH}}. \tag{7}$$

For a GJ consisting of N GJ channels, probability that there are $n_{\text{HH}}, n_{\text{HL}}$, and n_{LH} GJ channels in HH, HL, and LH states, respectively, is found by the multinomial distribution function given by

$$Pr\{G_{\text{gj}}(V_j)\} = N!\frac{p_{\text{HH}}^{n_{\text{HH}}}\cdot p_{\text{LH}}^{n_{\text{LH}}}\cdot p_{\text{HL}}^{n_{\text{HL}}}}{n_{\text{HH}}!\cdot n_{\text{LH}}!\cdot n_{\text{HL}}!}. \tag{8}$$

Assume that a GJ includes N GJ channels and they are distributed such that the number of the GJ channels in HH, HL, and LH states are $n_{\text{HH}}, n_{\text{HL}}$, and n_{LH}, respectively. Then, the total number of different combinations of $n_{\text{HH}}, n_{\text{HL}}$, and n_{LH} satisfying $n_{\text{HH}} + n_{\text{LH}} + n_{\text{HL}} = N$ can be found in the following manner. First, the selection of $n_{\text{HH}} = N, n_{\text{HL}} = 0$, and $n_{\text{LH}} = 0$ gives one combination. Second, for $n_{\text{HH}} = N - 1$,

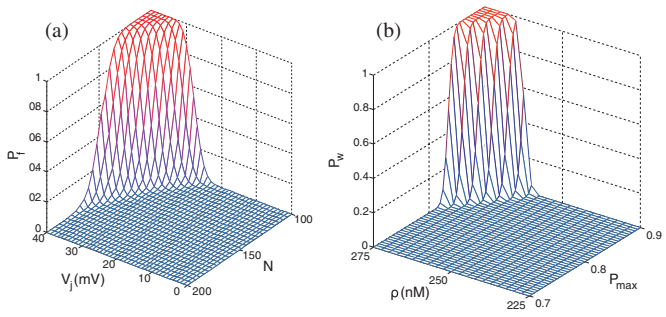

Fig. 2. (a) P_f plot with respect to V_j and the total number of the GJ channels in a GJ, N. (b) P_w plot with respect to ρ and $P_{\max}$.

there are two possible combinations: $n_{\rm HL}=0, n_{\rm LH}=1$ and $n_{\rm HL}=1, n_{\rm LH}=0$. Next, for $n_{\rm HH}=N-2$, there are three possible combinations: $n_{\rm HL}=0, n_{\rm LH}=2, n_{\rm HL}=1, n_{\rm LH}=1$, and $n_{\rm HL}=2, n_{\rm LH}=0$. If we continue in a similar way, for $n_{\rm HH}=0$, there are $(N+1)$ combinations. Thus, the total number of different combinations is given by $1+2+3+\cdots+(N+1)=\frac{1}{2}(N+1)(N+2)$. For each combination, the total conductance value and the probability of the corresponding combination is given in (7) and (8), respectively. We use MATLAB to obtain the probability mass function of the total conductance of a GJ having total N GJ channels by evaluating all possible channel state combinations and the corresponding probabilities.

Since the propagation of the AP fails when the GJ conductance value, $G_{\rm gj}(V_j)$, is less than the critical conductance value, $G^*_{\rm gj}$, we can find the probability of the propagation failure, denoted by P_f, using the probability mass function of the GJ conductance as follows:

$$P_f = Pr\{G_{\rm gj}(V_j) < G^*_{\rm gj}\} \tag{9}$$

where the critical conductance is the reciprocal of the critical resistance, $G^*_{\rm gj}=1/R^*_{\rm gj}$. The failure probability P_f depends on several parameters such as the critical GJ conductance $G^*_{\rm gj}$, the junctional voltage V_j, and the number of the GJ channels N, as clearly observed in (4), (8), and (9). In Fig. 2(a), the variation of P_f with N and V_j is shown.

D. Spontaneous Action Potential Initiation

The AP generation can be triggered in the absence of a stimulus due to some abnormalities of cardiomyocytes. Although normal and healthy ventricular cardiomyocytes do not exhibit such spontaneous generation of the AP, we incorporate the spontaneous AP generation into the GJ communication model considering diseased cardiomyocytes. The spontaneous AP initiation in a cardiomyocyte can be triggered by the $\rm Ca^{2+}$ release units (CRUs) of the sarcoplasmic reticulum [17]. If a CRU fires, it emits a $\rm Ca^{2+}$ ion spark into the cytoplasm of the cardiomyocyte. The emitted $\rm Ca^{2+}$ ions increase the membrane potential of the cardiomyocyte. Therefore, if the membrane potential becomes greater than a threshold due to the released $\rm Ca^{2+}$ ions by CRUs, an AP is triggered in the cardiomyocyte without an external stimulus. The probability that a CRU fires in the time duration T_s is

$$P_s = 1-\exp\left(-\frac{P_{\max}\rho^n}{K^n+\rho^n}T_s\right) \tag{10}$$

where $P_{\max}$ is the maximum probability of $\rm Ca^{2+}$ spark occurrence/CRU/unit time, ρ is the free $\rm Ca^{2+}$ molar concentration in the cytoplasm, K is the $\rm Ca^{2+}$ sensitivity parameter, and n is the Hill coefficient [17]. Let the number of the CRUs that fire in time T_s be m. Assuming the CRUs are independent of each other, m is distributed by the binomial probability distribution as $m\sim \mathrm{B}(M,P_s)$ where M is the total number of the CRUs in a cardiomyocyte. That is,

$$\Pr\{m \text{ sparks}\} = \binom{M}{m} P_s^m\,(1-P_s)^{M-m}\,. \tag{11}$$

Since M is a large number, we can use the Gaussian approximation of the binomial distribution given in (11) as $m\sim\mathcal{N}(MP_s, MP_s(1-P_s))$.

The number of $\rm Ca^{2+}$ sparks should be large enough to initiate an AP. In the GJ communication model, we use the half of the number of the CRUs as the required number of sparks to trigger an AP in T_s duration. Thus, the probability of an AP initiation without any stimulus, denoted by P_w, is

$$P_w = \Pr\left\{\frac{M}{2}<m\right\} = Q\left(\frac{(M/2)-MP_s}{MP_s(1-P_s)}\right) \tag{12}$$

where $Q(\cdot)$ is the Q-function. Since the distribution of m is approximated by Gaussian distribution, we can use Q-function to describe the probability given in (12). In Fig. 2(b), P_w with respect to both ρ and $P_{\max}$ is plotted. An increase in $P_{\max}$ causes an increase in P_s. Thus, an increase in $P_{\max}$ causes an increase in the expected number of the emitted $\rm Ca^{2+}$ sparks which increases the probability of the initiation of an AP as seen in Fig. 2(b). Furthermore, since increasing the free $\rm Ca^{2+}$ concentration ρ in the cardiomyocyte cytoplasm increases P_s, an increase in ρ due to the $\rm Ca^{2+}$ concentration fluctuations increases the spontaneous AP initiation probability.

III. Information Theoretical Analysis of Gap Junction Communication Channel

For the information theoretical model, we consider two cases to figure out the transmission probabilities of the information from TC to RC. The first case is the failure of the AP transmission; that is, RC detects bit 0 while bit 1 is transmitted by TC. The probability of the first case is P_f given in (9). The second case is the initiation of the AP at RC in the absence of a stimulus caused by TC; that is, RC detects bit 1 while bit 0 is transmitted by TC. The probability of the second case is P_w given in (12). The AP propagation failure and the spontaneous AP initiation are caused by the noise factors that intrinsically arise in the GJ communication. The intrinsic noise factors are related to the stochastic nature of both the GJ channels and the CRUs. Therefore, the information theoretical channel model of the GJ communication includes the peculiar noises and the noise factors specific to the GJ communication.

The GJ communication channel exhibits memoryless Binary Asymmetric Channel (BAC) characteristics with On–Off

Keying (OOK) modulation based on the analysis that we introduced so far. Assume that X is the transmitted bit by TC and Y is the received bit by RC. Then, we define the AP transmission probability of TC as $P_{\rm AP}$, i.e.,

$$P(x) = \begin{cases} P_{\rm AP}, & \text{if } X = 1 \\ 1 - P_{\rm AP}, & \text{if } X = 0. \end{cases} \tag{13}$$

Using (13) and the channel transmission probabilities, the joint probability distribution of X and Y, denoted by $P(x, y)$, is

$$P(x,y) = \begin{cases} (1-P_{\rm AP})(1-P_w), & \text{if } (X=0, Y=0) \\ (1-P_{\rm AP})P_w, & \text{if } (X=0, Y=1) \\ P_{\rm AP}P_f, & \text{if } (X=1, Y=0) \\ P_{\rm AP}(1-P_f), & \text{if } (X=1, Y=1). \end{cases} \tag{14}$$

The joint distribution $P(x, y)$ expresses the probability of that the observed output symbol is y and the transmitted symbol is x. The mutual information between X and Y denoted by $I(X;Y)$ is given in [18] as follows:

$$I(X;Y) = \sum_{x,y} P(x,y) \log_2 \frac{P(x,y)}{P(x)P(y)} \tag{15}$$

where $P(y)$ is the probability distribution of Y. It is straightforward to obtain $P(y)$ using the joint distribution $P(x, y)$. The GJ communication channel capacity denoted by $C_{\rm gj}$ is the maximum value of the mutual information [18] and the capacity of the GJ communication channel is found as follows:

$$C_{\rm gj} = \max_{P(x)} I(X;Y) \tag{16}$$

where $H(\cdot)$ is the binary entropy function. The channel characteristics of the GJ communication varies with several parameters such as the number of the GJ channels, the membrane resistivity, and the cell length and radius. Since such physiological properties vary among individual organisms and even among different sites on the same heart, in the next section, we analyze the GJ communication channel characteristics with respect to several physiological parameters.

IV. Numerical Analysis

In this section, we present a numerical analysis of the GJ communication parameters namely the channel capacity, the propagation delay, and the information transmission rate to show how these parameters change with the properties of cardiomyocytes and GJs.

For the numerical analysis, we model the cardiomyocyte membranes using the model presented in [10]. The propagation of the AP is simulated in a three-cell network as illustrated in Fig. 1. A stimulus is applied to TC to initiate the AP propagation. After exciting TC, an AP propagates to RC through the GJ between TC and RC. Since the occurrence probabilities of the GJ channel states depend on the junctional voltage between cardiomyocytes, we simulate the AP propagation by using the expected value of the total GJ conductance. For discrete time steps $\Delta t = 0.01$ ms, the junctional voltage is found as the difference between the membrane voltages of TC and RC.

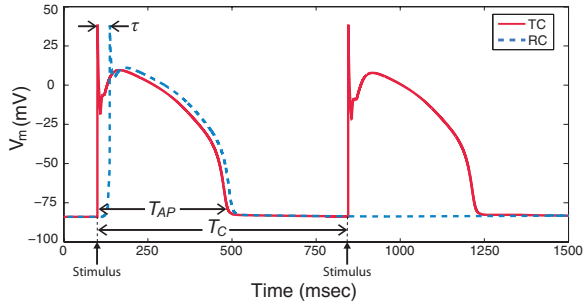

Fig. 3. Successful and a failed AP transmissions between TC and RC.

Then, at the obtained junctional voltage, the expected value of the total conductance is evaluated and replaced with the previous total conductance value assuming the total GJ conductance is constant for $\Delta t = 0.01$ ms. The expected value of the total conductance is

$$\mathrm{E}[G_{\rm gj}(V_j)] = \mathrm{E}[NG_{\rm ch}] = N(p_{\rm HH}G_{\rm HH} + p_{\rm HL}G_{\rm HL} + p_{\rm LH}G_{\rm LH}) \tag{17}$$

where the expectation of $G_{\rm ch}$ is found by using the probability mass function of the single GJ channel conductance in (6). After simulating the AP propagation by using the expectation of $G_{\rm gj}$ given in (17), we use the junctional voltage between TC and RC membranes for the channel capacity analysis. The junctional voltage attained from the simulation is used to evaluate $p_{\rm HH}, p_{\rm HL}$, and $p_{\rm LH}$ by using (4). Since the junctional voltage V_j is time varying and the probabilities depend on V_j, time average of the probabilities are used for (8).

An example of a successful and a failed transmission of APs between TC and RC can be seen in Fig. 3 which illustrates the membrane voltage changes of TC and RC over time. The channel propagation delay, denoted by τ, is the delay between the upstrokes of the APs generated in TC and RC. The AP pulse duration, denoted by $T_{\rm AP}$, is the time duration between the AP initiation instant and the time that the membrane potential is restored to its initial value. The cycle length, denoted by T_C, is the time between two successive stimuli that are applied to TC. That is, T_C is the signaling interval of TC. Therefore, the information transmission rate, denoted by R, is given by $R = 1/T_C$. In Fig. 3, the channel propagation delay τ, the AP pulse duration T_{AP}, and the cycle length T_C can be seen.

The numerical analysis of the mutual information expression is performed using (15). However, the numerical values of τ and $T_{\rm AP}$ are obtained from the simulation results of the AP generation model as performed in the physiological investigations [19]. For the analysis, we keep the following parameters constant at their typical physiological values which are $R_i = 250\,\Omega\cdot$cm, $R_e = 100\,\Omega\cdot$cm, $P_{\max} = 0.3, M = 30000, n = 1.6$ [17] and we assume $V_i = 5V_e$ and $T_s = T_{\rm AP}$.

A. Channel Capacity

1) Effect of Number of Gap Junction Channels: For the first analysis, we investigate the effect of the number of the GJ channels N in the GJ on the capacity of the GJ communication

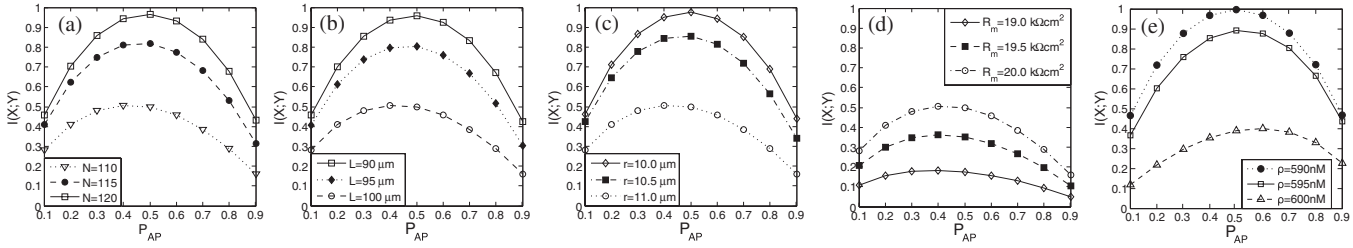

Fig. 4. $I(X;Y)$ in $bits$ for varying (a) number of the GJ channels, N, (b) length of the cardiomyocyte, L, (c) radius of the cardiomyocyte, r, (d) the membrane resistivity of the cardiomyocyte, R_m, and (e) the free Ca^{2+} concentration in the cytoplasm, ρ, with respect to P_{AP}.

channel C_{gj}. The analysis is carried out for the GJ between TC and RC for which the number of the GJ channels are varied from $N = 105$ to $N = 120$. We set the rest of the parameters as $L = 100\,\mu$ m, $r = 11\,\mu$ m, $R_m = 20\,\mathrm{k}\Omega \cdot \mathrm{cm}^2$ and $\rho = 100$ nM [10], [17]. A change in the number of the GJ channels clustered in the GJ affects directly the conductance of the GJ. That is, a lower number of the GJ channels results in a smaller conductance value which causes P_f to become larger as shown in Fig. 2(a). Therefore, the capacity of the GJ communication channel decreases with an decrease in N as seen in Fig. 4(a). The channel capacity of the GJ communication designed for nanodevices can be increased with an increase in the number of the GJ channels.

2) Effect of Cardiomyocyte Length: In this analysis, we examine the GJ communication channel capacity variation with the length of cardiomyocytes, L. We change the value of L while keeping the other parameters constant for $N = 110, r = 11\,\mu$m, $R_m = 20\,\mathrm{k}\Omega \cdot \mathrm{cm}^2$, and $\rho = 100$ nM [10], [17]. The change of the mutual information $I(X;Y)$ with varying AP generation probability of TC for different L values is shown in Fig. 4(b). The increase in the critical conductance value because of the increase in L yields an increase in P_f and hence a dramatical decrease in the capacity. The capacity reduction due to an increase in the length can be seen in Fig. 4(b). Thus, the capacity of the GJ communication of nanodevices can be improved by using short nanodevices.

3) Effect of Cardiomyocyte Radius: The effect of the radius of the cardiomyocytes on the GJ communication channel capacity is investigated by changing the value of the radius r, while setting the other parameters as $N = 110, L = 100\,\mu$m, $R_m = 20\,\mathrm{k}\Omega \cdot \mathrm{cm}^2$ and $\rho = 100$ nM [10], [17]. To understand change of the channel capacity with respect to r, we compute $I(X;Y)$ for different values of r with varying AP generation probability. The result of the analysis is shown in Fig. 4(c). The capacity decreases significantly with increasing r. Thus, using thin nanodevices can increase the capacity the GJ communication between nanodevices.

4) Effect of Membrane Resistivity of Cardiomyocyte: We investigate the effect of the membrane resistivity R_m of cardiomyocytes on the GJ communication channel capacity. Only R_m value is changed and the other parameters are set to $N = 110, L = 100\,\mu$ m, $r = 11\,\mu$ m and $\rho = 100$ nM [10], [17]. The membrane resistivity plays a critical role for the AP initiation and the propagation as stated in Section II-A. An increase in R_m decreases the critical conductance value given in (2); therefore, increasing R_m yields a reduction in P_f and hence an increase in the channel capacity. The increase in the channel capacity because of the increase in R_m can be seen in Fig. 4(d). Hence, the channel capacity of the GJ communication designed for nanodevices can be increased by using membranes with high resistivity values.

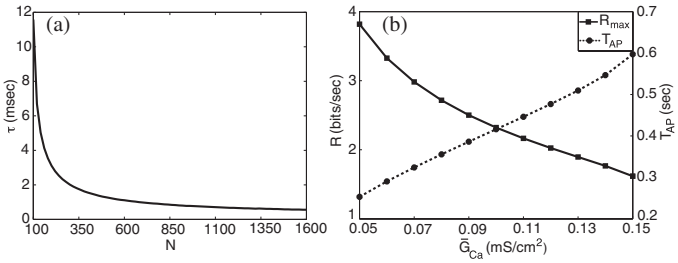

Fig. 5. (a) Channel propagation delay, τ, with respect to N. (b) Information transmission rate, R, and the AP duration, T_{AP}, with respect to the maximum conductance of the calcium channels, G_{Ca}.

5) Effect of Free Calcium Concentration: In this part, we investigate the effect of the free Ca^{2+} concentration ρ in the cytoplasm of the cardiomyocytes on the GJ communication channel capacity. In this analysis, we use the parameter values as $N = 1000, L = 100\,\mu$m, $r = 11\,\mu$m and $R_m = 20\,\mathrm{k}\Omega \cdot \mathrm{cm}^2$ [10]. In Fig. 4(e), the mutual information $I(X;Y)$ is shown for different concentration ρ values. An increase in the free Ca^{2+} concentration increases the probability of the spontaneous AP wave initiation P_w as stated in Section II-D. Therefore, increasing the free Ca^{2+} concentration decreases the capacity of the GJ communication channel C_{gj}.

B. Channel Propagation Delay

An AP pulse transmitted by TC to RC propagates through the GJ channels between TC and RC. During the AP propagation, the membrane voltage changes with time as shown in Fig. 3. As illustrated in the figure, there is a propagation delay τ. In Fig. 5(a), variation of the propagation delay with respect to the number of the GJ channels is shown. We use the typical physiological values for the remaining parameters which are $L = 100\,\mu$ m, $r = 11\,\mu$m, $R_m = 20\,\mathrm{k}\Omega \cdot \mathrm{cm}^2$ and $\rho = 100$ nM [10], [17]. The delay of the AP propagation from TC to RC decreases with increasing the number of the GJ channels. The

delay shows an abrupt decrease for increasing N from 100 to 300, and further increasing N causes the delay to decrease slowly. Consequently, we can say that further increasing N saturates the channel propagation delay to the propagation delay of the cytoplasm of the cardiomyocyte, i.e., the effect of discreteness of the cardiac fiber due to the GJ connections diminishes.

C. Information Transmission Rate

Assuming the cycle length is the same as the AP duration, i.e., $T_C = T_{\rm AP}$, the information transmission rate, R, in bits/s for the GJ communication is given as $R = 1/T_{\rm AP}$ where T_C and $T_{\rm AP}$ are the cycle length and the AP duration, respectively, as shown in Fig. 3. In Fig. 5(b), $T_{\rm AP}$ and R with respect to the maximum conductance of the calcium channels, denoted by $\bar{G}_{\rm Ca}$, is shown. $T_{\rm AP}$ variation for different $\bar{G}_{\rm Ca}$ values is found from the simulation results of the cardiac AP model in [10] and the variation of R for different $\bar{G}_{\rm Ca}$ values is obtained accordingly. In this part, we fix the parameters as $N = 1000, L = 100\,\mu$ m, $r = 11\,\mu$ m, $R_m = 20\,\Omega \cdot {\rm cm}^2$, and $\rho = 100$ nM [10], [17]. According to Fig. 5(b), T_m increases and R decreases with an increase in $\bar{G}_{Ca}$. Although increasing R is a desired objective in the classical communication, for the GJ communication, an increase in R due to the reduced $\bar{G}_{\rm Ca}$ may cause several arrhythmias.

V. Gap Junction Communication Channel Parameters and Cardiac Diseases

Since the GJ communication channel failures and deficiencies cause several disorders in the synchronous propagation of the APs and hence arrhythmias in the heart, in this section, we investigates the relation between GJ communication channel parameters and cardiac diseases. The numerical analysis shows that a decrease in the GJ coupling due to a reduction in the total number of the GJ channels clustered in a GJ causes capacity of the channel to decrease. According to results of investigations of heart diseases, a reduced GJ coupling leads to several heart diseases such as sudden death due to spontaneous ventricular arrhythmia [20] or an increase in incidence of ventricular tachycardias [21]. Thus, the reduction in the channel capacity due to the reduced GJ coupling is related with the increased incidence of the cardiac diseases.

In the GJ communication, the channel capacity decreases with an increase in the length of the cardiomyocyte, L, as shown in Fig. 4(b). The study presented in [22] investigates effects of the structural properties of cardiomyocytes on ischemic cardiomyopathy (ICM) and the results show that the length of cardiomyocytes is significantly longer in patients with ICM. We can say that a reduction in the capacity of the GJ channel causes more erroneous transmission of the information; as a result, the coordination between cardiomyocytes decreases and the cardiac tissue becomes diseased. Hence, a decrease in the channel capacity and an increase in the occurrence of ICM due to an increase in L are correlated.

The channel capacity of the GJ communication decreases with an increase in the radius of cardiomyocytes as illustrated in Fig. 4(c). The results of the study presented in [23] reveal that the radius of cardiomyocytes is significantly longer in hypertensive patients compared to normal subjects. That is, an increase in the radius of cardiomyocytes causes both a decrease in the channel capacity and an increase in the occurrence of hypertensive disease. Thus, the decrease in the channel capacity due to the increase in the cell radius is correlated with the increase in the incidence of the hypertension. The numerical analysis also shows that a reduction in the membrane resistivity decreases the channel capacity of the GJ communication as seen in Fig. 4(d). According to an analysis presented in [24], a decrease in the cardiomyocyte membrane resistivity is related to the impairment of the impulse propagation and it can cause severe cardiac arrhythmias. Hence, the reduction in the channel capacity due to the reduced membrane resistivity is accompanied with the cardiac arrhythmia.

From the numerical analysis, we observe that the GJ communication channel capacity decreases with an increase in the free $\rm Ca^{2+}$ concentration inside the cytoplasm of the cardiomyocytes as seen in Fig. 4(e). The free $\rm Ca^{2+}$ concentration overload causes several triggered arrhythmias such as delayed-afterdepolarizations (DADs) and early-afterdepolarizations (EADs) [25]. Furthermore, these triggered arrhythmias are major initiators of ventricular tachycardia which is an immediate precursor of ventricular fibrillation and a major cause of sudden death by heart failure [25]. Thus, the GJ communication channel capacity reduction due to the increased free $\rm Ca^{2+}$ concentration inside the cytoplasm is correlated with the increased occurrence of the ventricular tachycardia.

According to the results of the AP propagation delay analysis, an increase in the number of the GJ channels decreases the propagation delay as shown in Fig. 5(a). However, a decrease in N causes the propagation delay to increase and it is accompanied with a decrease in the channel capacity. That is, a decrease in the number of the GJ channels increases the propagation delay and decreases the channel capacity. As stated previously, the reduction of the GJ coupling due to the decrease in the number of GJ channel N causes several cardiac diseases. Therefore, it can be concluded that the AP propagation delay between cardiomyocytes is higher for the cases of the spontaneous ventricular arrhythmia [20] and the ventricular tachycardia [21].

The results of the numerical analysis show that a decrease in the maximum calcium channel conductance $\bar{G}_{Ca}$ increases the information transmission rate between TC and RC. At higher transmission rates, each received AP pulse also leads the RC to contract and relax at higher rates due to the excitation-contraction coupling property of cardiomyocytes. Therefore, since heart cannot support very high beating rates, an increase in R causes several arrhythmias. In [26], heart rates $>$100 beats/min are referred to as tachycardia causing the heart to be arrhythmic. Furthermore, prolongation of the AP duration, $T_{\rm AP}$, is a reason of the development of EADs causing a number of arrhythmias in the heart including long-QT syndrome and heart failure [27]. As a result, we can say that both very low and very high rate R increase the occurrence of the cardiac diseases stated previously.

Based on the observations stated previously, the most important deductions are those in diseased myocardium, the channel capacity of the GJ communication is lower and the propagation

delay is higher than for the case of healthy myocardium. Furthermore, the causes of very high or very low information transmission rates contribute to the occurrence of cardiac diseases. As a result, the information theoretical analysis of the GJ communication may provide valuable insights into causes of the cardiac diseases. The channel capacity, the channel propagation delay, and the transmission rate can be used as metrics for investigation, prediction, diagnosis, and treatment of several cardiac diseases in nanomedicine. These parameters can be measured and monitored by using multiple intrabody nanodevices and nanosensors communicating with cardiomyocytes via GJ channels. In addition, the information theoretical analysis of the GJ communication can be used for simulation tools of drug tests to confirm reliability of drugs. Hence, diagnosis and treatment techniques of cardiac diseases using the information theoretical model of the GJ communication stands as a promising application of the nanomedicine.

VI. Conclusion

In this study, we model the GJ communication channel between cardiomyocytes from the information theoretical perspective for the first time in the literature. The results of the numerical analysis of the GJ communication channel parameters show that the channel model presented in this paper can be used to get new insights into reasons of the cardiac diseases and hence diagnose and treat these diseases with the advances in nanomedicine. Furthermore, the numerical results reveal that the capacity of the GJ communication designed for nanodevices can be improved using the GJ communication model presented in this study.

References

[1] S. Hiyama, Y. Moritani, T. Suda, R. Egashira, A. Enomoto, M. Moore, and T. Nakano, "Molecular Communication," presented at the Nano Science and Technology Institute Nanotech., Anaheim, CA, 2005.

[2] M. Gregori and I. F. Akyildiz, "A new nanonetwork architecture using flagellated bacteria and catalytic nanomotors," *IEEE JSAC*, vol. 28, no. 4, pp. 612–619, May 2010.

[3] I. F. Akyildiz, F. Brunetti, and C. Blazquez, "Nanonetworks: A new communication paradigm," *Comput. Netw.*, vol. 52, no. 12, pp. 2260–2279, 2008.

[4] R. A. Freitas, *Nanomedicine, Vol. I: Basic Capabilities*. Austin, Texas: Landes Bioscience, 1999.

[5] L. P. Giné and I. F. Akyildiz, "Molecular communication options for long range nanonetworks," *Comput. Netw.*, vol. 53, no. 16, pp. 2753–2766, Nov. 2009.

[6] M. Kuscu and O. B. Akan, "A physical channel model and analysis for nanoscale molecular communications with förster resonance energy transfer," *IEEE Trans. Nanotechnol.*, vol. 11, no. 1, pp. 200–207, Jan. 2012.

[7] N. M. Kumar and N. B. Gilula, "The gap junction communication channel," *Cell*, vol. 84, pp. 381–388, 1996.

[8] T. Nakano T. Suda, T. Koujin, T. Haraguchi and Y. Hiraoka, "Molecular communication through gap junction channels," *Trans. Comput. Syst. Biol. X*, vol. 5410, pp. 81–99, 2008.

[9] G. Sohl and K. Willecke, "Gap junctions and the connexin protein family," *Cardiovasc. Res.*, vol. 62, pp. 228–232, 2004.

[10] C. H. Luo and Y. A. Rudy, "A dynamic model of the cardiac ventricular action potential—Part I: Simulations of ionic currents and concentration changes," *Circ. Res.*, vol. 74, pp. 1071–1096, 1994.

[11] J. P. Keener, "The effects of discrete gap junction coupling on propagation in myocardium," *J. Theor. Biol.*, vol. 148, pp. 49–82, 1991.

[12] G. W. Beeler and H. Reuter, "Reconstruction of the action potential of myocardial fibres," *J. Physiol.*, vol. 268, pp. 177–210, 1977.

[13] S. Baigent, S. Jaroslav, and A. Warner, "Modeling the effect of gap junction nonlinearities in systems of coupled cells," *J. Theor. Biol.*, vol. 186, pp. 223–239, 1997.

[14] F. F. Bukauskas, A. Bukauskiene, M. V. L. Bennett, and V. K. Verselis, "Gating properties of gap junction channels assembled from connexin43 and connexin43 fused with green fluorescent protein," *Biophys. J.*, vol. 81, pp. 137–152, 2001.

[15] V. Valiunas, R. Weingart, and P. R. Brink, "Formation of heterotypic gap junction channels by connexins 40 and 43," *Circ. Res.*, vol. 86, pp. E42–E49, 2000.

[16] H. Z. Wang, J. Li, L. F. Lemanski, and R. D. Veenstra, "Gating of mammalian cardiac gap junction channels by transjunctional voltage," *Biophys. J.*, vol. 63, pp. 139–151, 1992.

[17] L. T. Izu, W. G. Wier, and C. W. Balke, "Evolution of Cardiac Calcium Waves from Stochastic Calcium Sparks," *Biophys. J.*, vol. 80, pp. 103–120, Jan. 2001.

[18] C. E. Shannon, "A mathematical theory of communication," *Bell Syst. Tech. J.*, vol. 27, pp. 379–423, Jul. 1948.

[19] S. Rohr, "Role of gap junctions in the propagation of the cardiac action potential," *Cardiovasc. Res.*, vol. 62, pp. 309–322, 2004.

[20] D. E. Gutstein, G. E. Morley, H. Tamaddon, D. Vaidya, M. D. Schneider, J. Chen, K. R. Chien, H. Stuhlmann, and G. I. Fishman, "Conduction slowing and sudden arrhythmic death in mice with cardiac-restricted inactivation of connexin 43," *Circ. Res.*, vol. 88, pp. 333–339, 2001.

[21] D. L. Lerner, K. A. Yamada, R. B. Schuessler, and J. E. Saffitz, "Accelerated onset and increased incidence of ventricular arrhythmias induced by ischemia in Cx43-deficient mice," *Circuits*, vol. 101, pp. 547–552, 2000.

[22] A. M. Gerdes, S. E. Kellerman, J. A. Moore, K. E. Muffly, L. C. Clark, P. Y. Reaves, K. B. Malec, P. P. McKeown, and D. D. Schocken, "Structural remodeling of cardiac myocytes from patients with chronic ischemic heart disease," *Circuits*, vol. 86, pp. 426–430, 1992.

[23] K. Amann, M. Breitbach, E. Ritz, and G. Mall, "Myocyte/capillary mismatch in the heart of uremic patients," *J. Amer. Soc. Nephrol.*, vol. 9, pp. 1018–1022, 1998.

[24] W. C. D. Mello, "Cell swelling, impulse conduction, and cardiac arrhythmias in the failing heart. Opposite effects of angiotensin II and angiotensin (1–7) on cell volume regulation," *Mol. Cell. Biochem.*, vol. 330, pp. 211–217, 2009.

[25] D. M. Bers, "Calcium and cardiac rhythms: Physiological and pathophysiological," *Circ. Res.*, vol. 90, pp. 14–17, 2002.

[26] J. T. Nguyen, X. Li, and F. Lu, "The electrocardiogram and clinical cardiac electrophysiology," in *Proc. Card. Electrophysiol. Methods Models*, 2010, pp. 91–116.

[27] J. K. Donahue, M. Strom, and I. D. Greener, "Introduction to translational research," in *Proc. Card. Electrophysiol. Methods Models*, 2010, pp. 441–455.

Deniz Kilinc (S'12) received the B.Sc. degree in electrical and electronics engineering from Middle East Technical University, Ankara, Turkey, in 2011. He is currently working toward the M.Sc. degree from the Department of Electrical and Electronics Engineering , Koc University, Istanbul, Turkey.

He is currently a Research Assistant in the Next-Generation and Wireless Communication Laboratory, Istanbul. His current research interests include nanoscale communication, intrabody communication, and detection and estimation theory.

Ozgur B. Akan (M'00–SM'07) received the Ph.D. degree in electrical and computer engineering from the Broadband and Wireless Networking Laboratory, School of Electrical and Computer Engineering, Georgia Institute of Technology, Atlanta, in 2004.

He is currently a Full Professor with the Department of Electrical and Electronics Engineering, Koc University and the Director of the Next-Generation and Wireless Communications Laboratory. His current research interests include wireless communications, nanoscale and molecular communications, and information theory.

Dr. Akan is currently the General Cochair of ACM Mobicom 2012, IEEE MoNaCom 2012, and the TPC Cochair of IEEE ISCC 2012. He is an Associate Editor of the IEEE Transactions on Vehicular Technology, *International Journal of Communication Systems*, and *Nano Communication Networks Journal*.